

## New Limit on Neutrinoless Double $\beta$ Decay in $^{136}\text{Xe}$ with a Time Projection Chamber

H. T. Wong,<sup>(1),(a)</sup> F. Boehm,<sup>(1)</sup> P. Fisher,<sup>(1),(b)</sup> K. Gabathuler,<sup>(2)</sup> H. E. Henrikson,<sup>(1)</sup> D. A. Imel,<sup>(1)</sup>  
M. Z. Iqbal,<sup>(1),(c)</sup> V. Jörgens,<sup>(3)</sup> L. W. Mitchell,<sup>(3),(d)</sup> B. M. O'Callaghan-Hay,<sup>(1)</sup> J. Thomas,<sup>(1),(e)</sup>  
M. Treichel,<sup>(3)</sup> J.-C. Vuilleumier,<sup>(3)</sup> and J.-L. Vuilleumier<sup>(3)</sup>

<sup>(1)</sup>Norman Bridge Laboratory of Physics, California Institute of Technology, Pasadena, California 91125

<sup>(2)</sup>Paul Scherrer Institute, 5232 Villigen, Switzerland

<sup>(3)</sup>Institut de Physique, A.-L. Breguet 1, 2000 Neuchâtel, Switzerland

(Received 17 May 1991; revised manuscript received 5 August 1991)

A xenon time projection chamber with an active volume of 207 L has been built to study neutrinoless double  $\beta$  decay in  $^{136}\text{Xe}$ . Data were taken in the Gotthard Underground Laboratory, with 5 atm of xenon enriched to 62.5% in  $^{136}\text{Xe}$ . From 3380 h of data, no evidence has been found for the  $0\nu 0^+ \rightarrow 0^+$  transition. Half-life limits of  $T_{1/2}^{0\nu} > 2.5(4.9) \times 10^{23}$  yr in the mass-mechanism mode and  $T_{1/2}^{0\nu} > 1.7(3.2) \times 10^{23}$  yr in the right-handed-current mode, at the 90(68)% C.L., were derived. An upper limit for the Majorana neutrino mass parameter was deduced.

PACS numbers: 23.40.Bw, 14.60.Gh, 27.60.+j

It is well known that neutrinoless double  $\beta$  decay provides a sensitive probe for lepton-number violation and, in particular, Majorana neutrino mass as well as right-handed weak currents [1]. The implications of this so far unobserved nuclear decay have stimulated intense experimental efforts in recent years [2]. Experiments on  $^{76}\text{Ge}$  have produced the most stringent limits so far [3]. Owing to the uncertainties in the nuclear-matrix-element calculations [4], it is important that other isotopes are studied as well. In this Letter, we report on a double- $\beta$ -decay experiment with  $^{136}\text{Xe}$ , using a time projection chamber.

The isotope  $^{136}\text{Xe}$  is suitable for double- $\beta$ -decay studies. The  $0\nu$  transition energy (2.48 MeV) is large compared to other candidate isotopes, leading to an enhancement of the phase-space factor and decay rate. In addition, xenon is a good proportional counter and drift gas, and thus can act as both source and detector. The natural abundance (8.9%) is appreciable, and xenon enriched in  $^{136}\text{Xe}$  can be obtained [5] at a relatively modest price. Experimental searches for double  $\beta$  decay in  $^{136}\text{Xe}$  have been carried out by groups from Moscow [6] and Milano [7], using a high-pressure ionization chamber and a multi-element proportional counter, respectively.

We have built a time projection chamber (TPC) [8] to study double  $\beta$  decay in  $^{136}\text{Xe}$ , in both the  $0\nu$  and  $2\nu$  channels [9]. The Monte Carlo studies [10], basic design [11], electronics [12], and data-acquisition system [13] of the TPC have been described elsewhere. A schematic diagram of the experimental setup is shown in Fig. 1. The TPC has a cylindrical active volume of 207 L. The operating pressure is 5 bars, with an admixture of 3.9% methane to increase the drift velocity (to  $1.36 \text{ cm } \mu\text{s}^{-1}$ ) and to suppress diffusion of the secondary electrons [14]. Gas purity is maintained at a 0.1-ppm level in electronegative contaminants [9]. Xenon enriched to 62.5%  $^{136}\text{Xe}$  is used [5], giving a total of  $1.6 \times 10^{25}$   $^{136}\text{Xe}$  atoms in the active volume. According to Monte Carlo calculations [9,10], the probabilities for a double- $\beta$ -decay event at 2.5 MeV to be completely contained within the active volume

are 25% and 21% for  $0\nu\beta\beta$  induced by the mass mechanism and by right-handed weak couplings, respectively. The difference is mainly due to the difference in energy distribution between the two electrons in the two modes [15]. There are 168 readout channels, with 3.5-mm pitch, in each of the  $X$  and  $Y$  axes. The time evolution of the signals, recorded in 500-ns bins, gives trajectory information in the  $Z$  direction. The energy of an event is measured from the integration of the anode signals over the drift time of 51  $\mu\text{s}$ .

To minimize the radioactive background, the chamber has been built with OFHC (oxygen-free high-conductivity) copper with a thickness of 5 cm, while all other components have been selected for their trace radioactivity with a low-background germanium detector. The copper vessel is further shielded by 20–30 cm of lead. The experiment is being conducted at the Gotthard Underground Laboratory, with a 3000-m water-equivalent overburden which attenuates the muon flux by a factor of  $10^6$ .

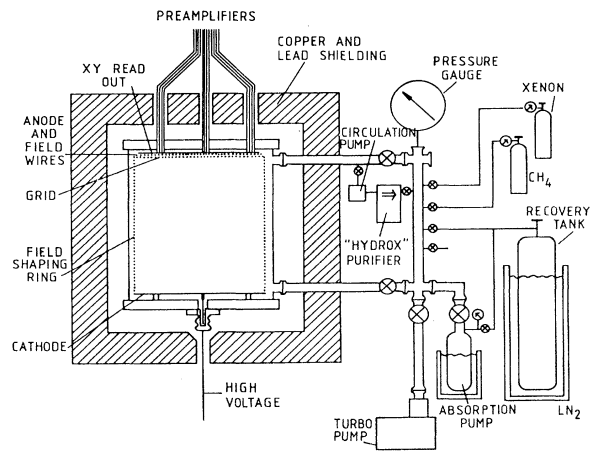


FIG. 1. A schematic diagram of the time projection chamber with the associated setup.

The track reconstruction capability of the TPC provides a powerful means of background rejection. A double  $\beta$  decay is identified as a continuous trajectory with characteristic "end features": high charge depositions (charge "blobs") due to enhanced  $dE/dx$  at low energy, and large-angle multiple scattering (that is, staggered trajectories), at both ends. Owing to bremsstrahlung emissions, some of these events have small isolated charge depositions ( $< 150$  keV). The major background is from

pair production as well as single-electron events (due to the photoelectric effect, Compton scattering, or  $\beta$  decay) with the emission of energetic secondary ("delta") electrons at the beginnings of their trajectories.

Some typical events recorded by the TPC are shown in Figs. 2(a)–2(c). The  $XZ$  and  $YZ$  projections as well as the time evolution of the anode signals are displayed. The large black dots indicate signals above a second level threshold, corresponding to charge blobs. The TPC does

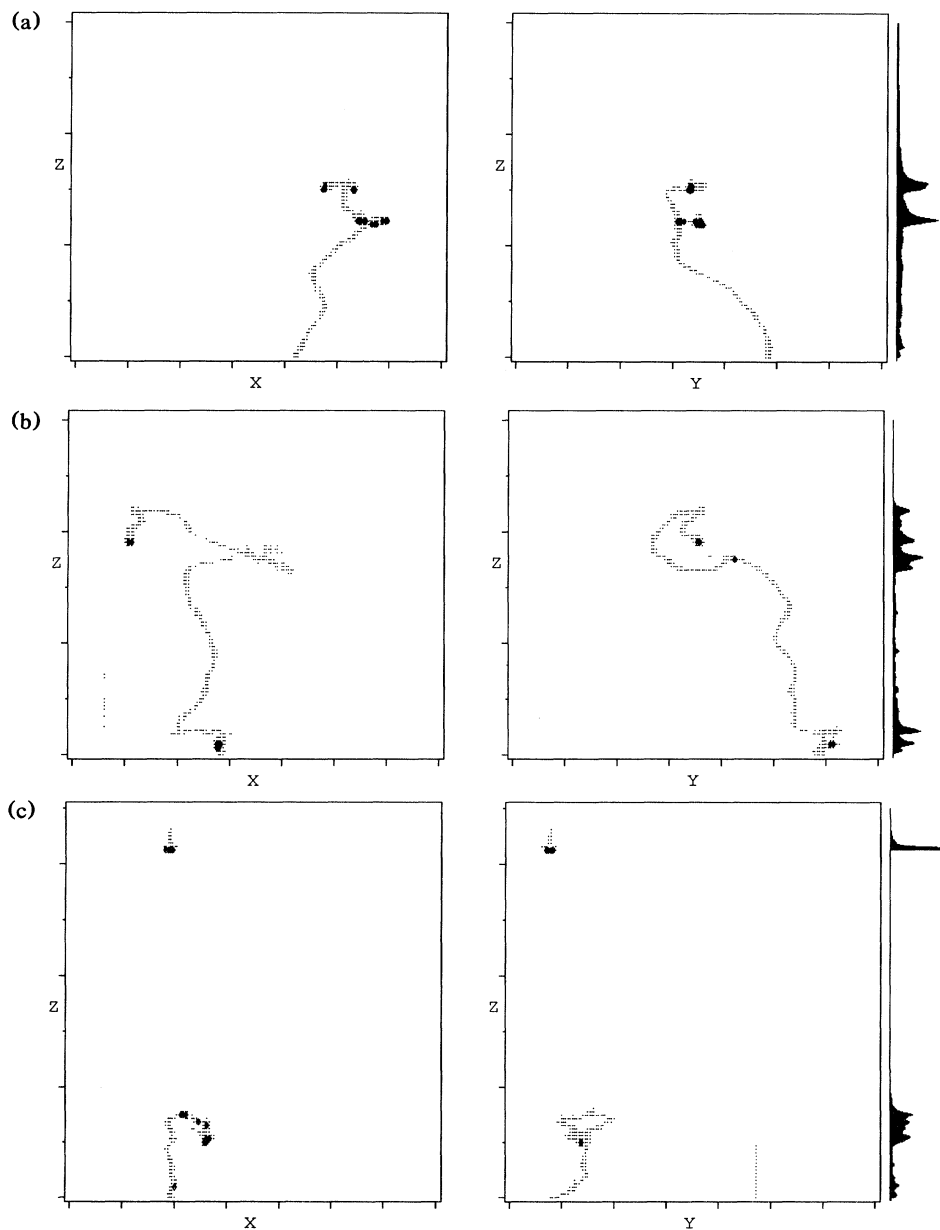


FIG. 2. Typical tracks recorded by the TPC with 5 atm of xenon. (a) Single electron; (b) two-electron candidate event; and (c)  $\beta$  decay followed by emission of an  $\alpha$  particle. In (a)–(c) the full range is 60 cm for both  $X$  and  $Y$ , while the  $Z$  calibration is 10.9 cm per unit.

not have a time-zero trigger; the  $Z=0$  in the figures corresponds to the first arrival of the signals. The full range for both  $X$  and  $Y$  is 60 cm. Calibration of the  $Z$  axis depends on the drift velocity of the secondary electrons. It is measured from the length of cosmic-ray muons traversing vertically through the detector. Typically, a few such events are recorded per day. The  $Z$  calibration is 10.9 cm per unit in the displayed figures, and the variation with time is less than 1%.

A typical single-electron event and a typical candidate for a two-electron event are depicted in Figs. 2(a) and 2(b). They are readily distinguishable by the features their trajectories exhibit at their ends (charge blobs and staggered trajectories). Figure 2(c) shows a  $\beta$  decay followed by the emission of an  $\alpha$  particle at the same  $(X, Y)$  coordinate 50  $\mu$ s later. This event is due to the cascade  $^{214}\text{Bi} \rightarrow ^{214}\text{Po} + e^- + \bar{\nu}_e$  ( $Q=3.28$  MeV,  $T_{1/2}=19.7$  min), followed by  $^{214}\text{Po} \rightarrow ^{210}\text{Pb} + \alpha$  ( $Q=7.8$  MeV,  $T_{1/2}=164$   $\mu$ s), and is evidence of trace radon emission in the system. Among the daughter nuclei of the radon isotopes from the  $^{238}\text{U}$  and  $^{232}\text{Th}$  chains, only this  $\beta$  decay has an end-point energy above 2.5 MeV. However, as demonstrated, this cascade can be singled out by looking for the  $\sim 100$ - $\mu$ s post-trigger  $\alpha$  activity after an initial single-electron event.

The energy resolution and calibration has been studied with various  $\gamma$  sources. A (10–15)% variation in charge multiplication across the effective area of the anode plane is observed. To correct for this effect, the anode plane is subdivided into 45 squares and a gain variation map is made from a measurement with a  $^{137}\text{Cs}$  source. The anode signals are then compensated for at each time bin, based on the  $(X, Y)$  coordinate of the event at that time. A notable improvement on the energy resolution of 14.8% and 6.6% FWHM at 511 and 1592 keV, respectively, is subsequently achieved. The energy spectrum for a  $^{232}\text{Th}$  source, after applying this gain correction, is shown in Fig. 3. The 1592-keV peak is due to double escape (pair production with the total escape of both 511-keV photons) from the incident  $\gamma$  rays of 2614 keV. The overall

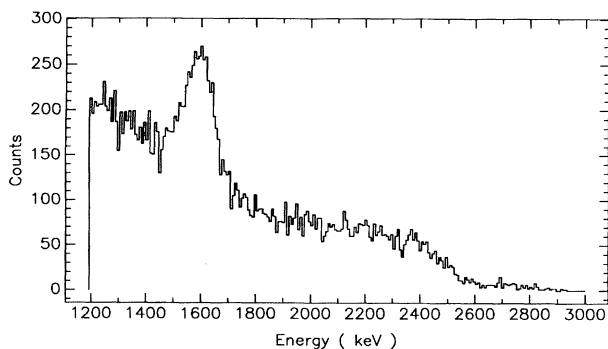


FIG. 3. Energy spectrum of a  $^{232}\text{Th}$  source. The prominent line is the double escape peak of the 2614-keV  $\gamma$  rays in  $^{208}\text{Pb}$ .

gain (combined effects of charge multiplication, gas-purity level, and electronics) is constant over the course of data taking to better than 2%. The energy calibration is linear in our range of interest, and is accurate to better than 2%.

The results of a total of 3380 h of data, with an energy threshold of 1.6 MeV, are presented in this Letter. The two-electron spectrum displayed in Fig. 4 is obtained as follows. An off-line software program identifies and rejects events due to  $\alpha$  particles, multiple tracks, cascades, uncontained events, and distinct single electrons, reducing the data size by a factor of 6. Remaining events are then scanned visually. The selection of two-electron events requires charge blobs and staggered trajectories at both ends of a continuous trajectory. Events with isolated charge depositions of more than 150 keV are rejected. For this analysis, those events with sharp vertices in the central portion of the trajectories (which might suggest pair production) are kept. With these analysis procedures, there are typically 36 times as many single-electron as two-electron events above 1.6 MeV. It can thus be deduced that the single-electron rejection efficiency of the TPC is at least 97%. The probabilities of a contained  $\beta\beta$  event surviving these cuts have been studied with Monte Carlo simulations and with a smaller data set where all events are scanned visually. They are 81% and 64% for the mass-mechanism and right-handed-current modes, respectively, at the  $0\nu$  transition energy. The contributing factors include topological ambiguities (e.g., a track retraces itself), detector effects (inactive or noisy electronics), and the asymmetric energy distribution between the two electrons. The last factor is the major contribution to the difference in the efficiencies between the two mechanisms [15].

As stated above, the measured energy resolution is 6.6% FWHM at 1.6 MeV. We adopt the conservative

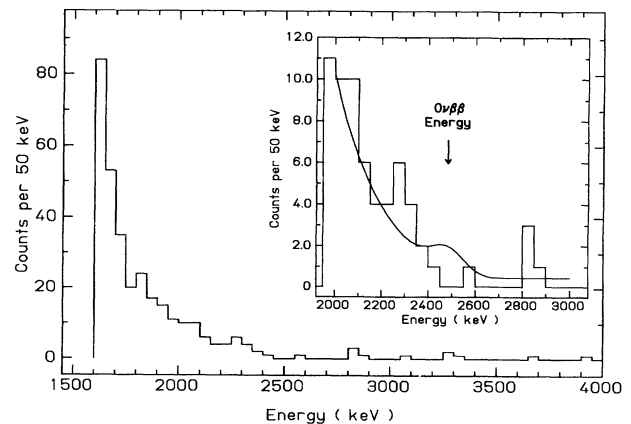


FIG. 4. Energy spectrum of two-electron candidate events, from 3380 h of data. The 90%-C.L. limit curve for a hypothetical  $0\nu$  peak at 2481 keV is represented by the solid line in the inset.

approach of taking this to be the resolution at the  $0\nu$  transition energy of 2.48 MeV. Based on Poisson statistics, the probability of a peak to be present at the transition energy is evaluated. Assuming an exponential background between 2000 and 2650 keV together with a constant background from 2650 to 3000 keV, we obtain an upper limit of 3.5(1.8) events for a hypothetical  $0\nu$  peak at a 90(68)% confidence level. Folding in the overall detector and analysis efficiencies [20% and 13% for the mass-mechanism and right-handed-current (RHC) modes, respectively], we obtain the following 90%-C.L. half-life limits:

$$T_{1/2}^{0\nu}(0^+ \rightarrow 0^+; \langle m_{\nu} \rangle) > 2.5 \times 10^{23} \text{ yr},$$

$$T_{1/2}^{0\nu}(0^+ \rightarrow 0^+; \text{RHC}) > 1.7 \times 10^{23} \text{ yr},$$

respectively. The corresponding 68% confidence limits are  $4.9 \times 10^{23}$  and  $3.2 \times 10^{23}$  yr, respectively. These numbers represent almost 1-order-of-magnitude improvement over existing limits [6,7]. The 90%-C.L. curve is folded onto the energy spectrum displayed in Fig. 4.

The limit for the Majorana neutrino mass parameter thus deduced depends on which nuclear-matrix-element calculation [4] one uses. Adopting the quasiparticle random-phase approximation by Engel, Vogel, and Zirnbauer [16] (and choosing  $\alpha'_1 = -375 \pm 15 \text{ MeV fm}^3$  which reproduces the measured  $2\nu\beta\beta$  half-lives in  $^{82}\text{Se}$ ,  $^{100}\text{Mo}$ , and  $^{130}\text{Te}$ ), the 90%-C.L. upper limit for the mass-mechanism mode ( $2.5 \times 10^{23}$  yr) implies

$$\langle m_{\nu} \rangle < 3.3\text{--}5.0 \text{ eV}.$$

This can be compared with  $\langle m_{\nu} \rangle < 2.4\text{--}4.7 \text{ eV}$ , derived from the most recent  $^{76}\text{Ge}$  results [3] ( $T_{1/2}^{0\nu} > 1.2 \times 10^{24}$  yr at the 90% C.L., with 3 yr of data) using the same calculation.

Data taking continues on this experiment in the Gotthard Laboratory. With the measured background level of 0.02 count per 100 keV per day ( $0.01 \text{ count keV}^{-1} \text{ kg}^{-1} \text{ yr}^{-1}$ ) in the  $0\nu$  energy range, we expect, with 1 yr of data, sensitivities of  $5 \times 10^{23}$  yr for  $T_{1/2}^{0\nu}(0^+ \rightarrow 0^+)$ , or 2.3–3.6 eV for  $\langle m_{\nu} \rangle$ . Studies of the  $2\nu\beta\beta$  channel will also be carried out.

The authors would like to thank Petr Vogel for many contributions and discussions, Val Telegdi for stimulating comments, and J.-P. Bourquin, C. Heche, D. Schenker, and the technical staff from Institut de Physique-Neuchâtel and Paul Scherrer Institute for assistance. This work is supported by the U.S. Department of Ener-

gy and the Fonds National Suisse pour la Recherche Scientifique.

(a)Correspondence address: Institut de Physique, A.-L. Breguet 1, 2000 Neuchâtel, Switzerland.

(b)Present address: Department of Physics and Astronomy, Johns Hopkins University, Baltimore, MD 21218.

(c)Present address: Bellcore, 331 Newman Springs Road, NVC 3X-239, Red Bank, NJ 07701.

(d)Present address: Department of Physics, Flinders University, Bedford Park, SA 5042, Australia.

(e)Present address: L-397, Lawrence Livermore National Laboratory, Livermore, CA 94550.

- [1] See, for example, F. Boehm and P. Vogel, *Physics of Massive Neutrinos* (Cambridge Univ. Press, Cambridge, 1987).
- [2] For a recent review, see M. K. Moe, in Proceedings of the Fourteenth International Conference on Neutrino Physics and Astrophysics, Geneva, 1990, edited by J. Panman and K. Winter [Nucl. Phys. B, Proc. Suppl. (to be published)].
- [3] D. O. Caldwell *et al.*, in Proceedings of the Fourteenth European Physical Society Conference on Nuclear Physics, Bratislava, 1990, edited by P. Povinec [J. Phys. G (to be published)]; F. Boehm *et al.*, in *Proceedings of the Twenty-Sixth Recontre de Moriond, Les Arcs, 1991*, edited by O. Fackler and J. Tran Thanh Van (Editions Frontières, Gif-sur-Yvette, 1991).
- [4] For a recent review, see T. Tomoda, Rep. Prog. Phys. **54**, 53 (1991).
- [5] Supplier: Monsanto Research Corporation (Mound, Oak Ridge).
- [6] A. S. Barabash *et al.*, Phys. Lett. B **223**, 273 (1989).
- [7] E. Bellotti *et al.*, Phys. Lett. B **221**, 209 (1989).
- [8] For an overview of the subject, see *The Time Projection Chamber*, edited by J. A. Macdonald, AIP Conf. Proc. No. 108 (AIP, New York, 1984).
- [9] H. T. Wong, Ph.D. thesis, Caltech, 1991 (unpublished).
- [10] M. Z. Iqbal, B. M. O'Callaghan, and H. T. Wong, Nucl. Instrum. Methods Phys. Res., Sect. A **253**, 278 (1987).
- [11] M. Z. Iqbal *et al.*, Nucl. Instrum. Methods Phys. Res., Sect. A **259**, 459 (1987).
- [12] M. Z. Iqbal, B. M. O'Callaghan, and H. T. Wong, Nucl. Instrum. Methods Phys. Res., Sect. A **263**, 387 (1988).
- [13] J. Thomas *et al.*, IEEE Trans. Nucl. Sci. **34**, 845 (1987).
- [14] M. Z. Iqbal *et al.*, Nucl. Instrum. Methods Phys. Res., Sect. A **243**, 459 (1986).
- [15] M. Doi, T. Kotani, and E. Takasugi, Prog. Theor. Phys. Suppl. **83**, 1 (1985).
- [16] J. Engel, P. Vogel, and M. R. Zirnbauer, Phys. Rev. C **37**, 731 (1988).